Pseudoscalar couplings in tt[over ⁻]H production at NLO+NLL accuracy

Alessandro Broggio, Andrea Ferroglia, Miguel C. N. Fiolhais, and António Onofre

Pseudoscalar couplings in $t\bar{t}H$ production at NLO+NLL accuracy

Alessandro Broggio[1], Andrea Ferroglia[2,3], Miguel C. N. Fiolhais[4,5], António Onofre[6]

[1] *Physik Department T31, Technische Universität München, James Franck-Straße 1, D-85748 Garching, Germany*
[2] *Physics Department, New York City College of Technology, The City University of New York, 300 Jay Street, Brooklyn, NY 11201 USA*
[3] *The Graduate School and University Center, The City University of New York, 365 Fifth Avenue, New York, NY 10016 USA*
[4] *Science Department, Borough of Manhattan Community College, City University of New York,*
199 Chambers St, New York, NY 10007, USA
[5] *LIP, Departamento de Física, Universidade de Coimbra, 3004-516 Coimbra, Portugal*
[6] *LIP, Departamento de Física, Universidade do Minho, 4710-057 Braga, Portugal*

We study the production of a Higgs boson in association to a top-antitop pair at the Large Hadron Collider. We show how precise predictions for the differential distributions with respect to the transverse momentum of the Higgs boson, to the invariant mass of the top-antitop-Higgs system and to the invariant mass of the top-antitop pair can provide useful information on the possible presence of a pseudoscalar component in the coupling of the top quark with the Higgs boson. We evaluate the production of a top-antitop pair and a Higgs boson to next-to-leading order in fixed order perturbation theory and we carry out the resummation of soft emission corrections to next-to-leading-logarithmic accuracy for the LHC operating at a center of mass energy of 13 TeV. We discuss how the shape of these distributions can be employed experimentally, making a physics case for the kinematic reconstruction of dilepton channels.

I. INTRODUCTION

At the Large Hadron Collider (LHC), the study of the associated production of a top-quark pair and a Higgs boson offers the unique opportunity of obtaining direct information on the Yukawa coupling of the top quark. Since in the Standard Model (SM) of particle physics the top quark is the particle which is predicted to have the strongest coupling with the Higgs boson, the study of this Yukawa coupling can prove important in the understanding of the electroweak symmetry breaking mechanism. In order to fully exploit the potential of the LHC in the study of this process, precise measurements, involving ideally the full kinematic reconstruction of the top pair and Higgs boson momenta, should be matched by (at least) equally precise theoretical predictions for measured observable quantities. For this reason, within the SM, higher order corrections to this process have been a subject of investigation for several years. Next-to-leading-order (NLO) QCD corrections were at first evaluated in [1–6]. Subsequently, these corrections were evaluated again in the process of developing and testing new tools for automated calculation of NLO corrections [7, 8]. The electroweak corrections to this process were studied in [9–12]. The associated production of a top pair and a Higgs boson, including the decay of the top quark and off-shell effects was evaluated to NLO in [13, 14].

The resummation of potentially large effects due to the emission of soft gluons in the final state was studied in [15–19]. In [16] a parton level Monte Carlo code was developed in order to evaluate the soft emission corrections to $t\bar{t}H$ production to next-to-next-to-leading logarithmic (NNLL) accuracy. The NNLL corrections were then matched to NLO calculations obtained by employing `MadGraph5_aMC@NLO` [20] (which we will indicate with `MG5_aMC` in the rest of this paper). In this way, within the SM, it was possible to obtain NLO+NNLL predictions for

the $t\bar{t}H$ total cross section as well as for several differential distributions which depend on the four momenta of the final state top quark, top antiquark and Higgs boson.

The cross section of the associated production of the Higgs boson with a top-quark pair at the LHC is of a few hundred femtobarn. Since this process has a huge background contamination stemming from $pp \to t\bar{t} + \text{jets}$ and other processes, it is easy to see that the associated $t\bar{t}H$ productions is extremely difficult to measure at the LHC. The ATLAS and CMS analysis teams have already obtained a combined best-fit value for the signal strength of $\mu = \sigma/\sigma_{\text{SM}} = 2.3^{+0.7}_{-0.6}$ [21–23]. The expected increase of integrated luminosity at the LHC, and further progress in the experimental techniques might make the the observation possible at run II.

It is of course also crucial to try to understand which kind of information about possible non-SM couplings of the top quark to the Higgs boson can become accessible when this process will be detected at the LHC. In particular, it is interesting to see if the Higgs boson couples to the top quark not only with a scalar coupling, but also through a pseudoscalar one. A comprehensive study of this aspect can be found in [24], where the CP properties of the top-quark Yukawa interaction are studied in the context of Higgs production in gluon fusion or in association with top quarks. In that work, NLO QCD preditions for $t\bar{t}H$ production within an Effective Field Theory approach of [25] are presented.

This works investigates the possible presence of a pseudoscalar component in the top-quark Yukawa coupling from a different perspective; in particular the purpose of this paper is twofold:

   a) We reconsider the role that the shape of some differential distributions can have in the study of a possible pseudoscalar component in the coupling of the Higgs boson to the top-quark, taking into account the possibility of a full experimental reconstruction

of the top, antitop and Higgs boson momenta.

b) We show that it is relatively straightforward to obtain precise, beyond NLO predictions for differential distributions which are sensitive to a pseudoscalar component in the top quark Yukawa coupling.

For this purpose, we consider the benchmark scenario described in Table 3 of [24], in which the coupling of the top-quark current to a "Higgs Boson" X_0 is described by the effective Lagrangian

$$\mathcal{L}_0^t = -\frac{m_t}{v} \, \overline{\psi} \left(\cos\alpha + i \sin\alpha \gamma_5 \right) \psi X_0 \,, \qquad (1)$$

where the angle α parameterizes the relative weight of the scalar and pseudoscalar couplings. In Eq. (1), m_t indicates the mass of the the top quark and v the vacuum expectation value. In the following we will identify X_0 with the SM Higgs boson H when we consider a purely scalar coupling ($\alpha = 0$) while we will use the notation $X_0 \to A$ when we consider a purely pseudoscalar coupling ($\alpha = \pi/2$). The part of the Lagrangian in Eq. (1) which is proportional to γ_5 is odd under a CP transformation. While Eq. (1) is not the most generic effective Lagrangian for this sector of the SM, it allows us to study in particular the effect of mixed scalar-pseudoscalar coupling on the shape of several differential distributions.

Experimentally, a full reconstruction of the momenta of the $t\bar{t}X_0$ final state is possible, and this allows one to measure distributions which are differential with respect to the momenta of the final state massive particles. Four of these distributions play an important role in this work: the differential distribution with respect $i)$ to the invariant mass of the three massive particles in the final state, $ii)$ to the transverse momentum of the X_0 boson, $iii)$ to the invariant mass of the top pair, and $iv)$ to the transverse momentum of the top quark. The shapes of these distributions, with the exception of the transverse momentum of the top quark, show significant differences between the pure scalar and pseudoscalar cases at generator level. Consequently they can be used to experimentally probe the pseudoscalar component. Even though parton showering, detector acceptance, event selection and reconstruction are expected to considerably degrade these specific distributions and their discriminant power [24], several studies strongly suggest that similar distributions involving full kinematic reconstruction can be measured [26, 27]. In addition, these same studies indicate that new interesting angular distributions and asymmetries can be defined from the reconstructed top quarks and Higgs boson in order to discriminate the signal from the main irreducible backgrounds in dileptonic decays in an extremely efficient way, even after event reconstruction. Besides the fact that the full kinematic reconstruction of $t\bar{t}X_0$ events is extremely challenging, due to the presence of two undetected neutrinos in the dilepton channel, results show that angular distributions involving the reconstructed top quarks and Higgs boson

and/or their decaying products are significantly different for the signal and the main irreducible backgrounds. A similar strategy can be implemented to probe the pseudoscalar component of the top quark Yukawa coupling, by exploring new distributions, highly sensitive to the mixing angle.

In order to obtain precise predictions for the associated production of a top pair and a X_0 boson we write a parton level Monte Carlo which includes the resummation of soft emission corrections in the partonic threshold limit defined by $z = M^2/\hat{s} \to 1$, where M is the invariant mass of the $t\bar{t}X_0$ final state and $\hat{s}$ is the partonic center of mass energy. The resummation of these corrections is carried to next-to-leading logarithmic (NLL) accuracy. Predictions to NLO+NLL accuracy for the total cross section and the four differential distributions listed above are obtained by matching the output of the parton level Monte Carlo with the NLO calculations obtained by using `MG5_aMC`.

The paper is structured as follows. In Section II we present predictions for the total cross section and differential distributions for $t\bar{t}X_0$ production considering the cases in which X_0 couples to the top quark as a scalar ($x_0 \to H$), pseudoscalar ($X_0 \to A$) and as a mixture of the two. In Section III we discuss how the measurement of these quantities can be employed to extract information about the coupling of X_0 with the top. Section IV contains our conclusions.

II.   CALCULATION AND RESULTS

The process of interest in this work is the associated production of a top pair and a boson X_0 which couples to the top quark according to the Lagrangian in Eq. (1). From the calculational point of view, this process is equivalent to the associated production of a top pair and a Higgs boson in the SM. The resummation of the latter process in the partonic threshold limit was studied in detail in [15, 16]. In particular, in [16] predictions for $t\bar{t}H$ production were obtained to NLO+NNLL accuracy. That calculation was carried out by means of an in-house parton level Monte Carlo code that was employed for the numerical evaluation of the resummation formula to NNLL accuracy. The NNLL calculations were then matched to NLO results obtained by using `MG5_aMC`. Our goal in this paper is to calculate to NLL accuracy the $t\bar{t}X_0$ production process of an arbitrary mixture of scalar and pseudoscalar coupling of X_0. We then match the results obtained to NLO calculations carried out by using the the model package for `MG5_aMC` developed for the work published in [24].

The resummation formula which we employ is derived along the lines of the one discussed in [16] for the SM case and of the ones obtained in [29, 30] for $t\bar{t}W$ and $t\bar{t}Z$ production, respectively. For this reason, we do not repeat a detailed description of the resummation formula and

of the resummation technique here[1]. We simply point out that in order to carry out the resummation to NLL accuracy one needs to evaluate the anomalous dimensions, soft functions and hard functions to LO only. The anomalous dimensions and the soft functions are identical to the ones employed in the SM calculation. The LO hard function for the quark-annihilation and gluon fusion partonic production channels can be readily obtained with a simple analytic calculation. The numerical evaluation of the resummed cross section is carried out in Mellin moment space, as it was done in [16, 29, 30]. Physical results are then obtained with a numerical inverse Mellin transform carried out by employing the *Minimal Prescription* to avoid problems related to the presence of the Landau pole [32].

When combining resummed calculations to fixed order calculations, it is important to avoid the double counting of terms included in both approaches. This is achieved through the procedure of "matching". In the case considered in this work, the matching procedure can be summarized in a schematic equation, which we write down here for the case of the total cross section:

$$\sigma^{\text{NLO+NLL}} = \sigma^{\text{NLO}} + \left[\sigma^{\text{NLL}} - \sigma^{\text{NLL expanded to NLO}}\right] \tag{2}$$

In Eq. (2) the terms within square brackets give contributions starting at NNLO.

Resummed calculations to a given logarithmic accuracy have a residual dependence on three non-physical scales: the factorization scale μ_f, which appears also in fixed order calculations, the soft scale μ_s which characterizes the soft gluon emission, and the hard scale μ_h which is the scale that characterizes the hard scattering. In addition, NLO calculations employed in the matching step also depend on the renormalization scale μ_r. Throughout this paper we set $\mu_f = \mu_r$. The hard and soft scales appear only in the resummed partonic cross section. The soft function evaluated at the scale μ_s and the hard function evaluated at the scale μ_h are free from large logarithms. By solving the Renormalization Group Equations satisfied by the soft and hard functions the partonic cross section is evolved to the factorization scale μ_f and then convoluted with the partonic luminosity. In fixed order calculations, the residual perturbative uncertainty associated to corrections at perturbative orders which are higher than the one considered in the calculation is estimated by varying the default choice for the factorization/renormalization scale by a factor of two. To be specific, if one indicates the default choice for the factorization scale with $\mu_{f,0}$, the scale is then varied in the interval $\mu_f \in [\mu_{f,0}/2, 2\mu_{f,0}]$; subsequently, the scale uncertainty affecting the fixed order result is taken to

be the interval included between the largest and smallest values of the observable obtained while varying the factorization scale. In resummed calculations, also the hard and soft scales are varied by a factor of two around their default value, indicated by $\mu_{s,0}$ and $\mu_{h,0}$ respectively: $\mu_s \in [\mu_{s,0}/2, 2\mu_{s,0}]$ and $\mu_h \in [\mu_{h,0}/2, 2\mu_{h,0}]$. The perturbative scale uncertainty affecting resummed calculations is estimated by varying separately the hard, soft, and factorization scales and by subsequently combining the uncertainties in quadrature. In particular, for any observable O (which can be the total cross section or the value of the differential cross section in a particular bin), one evaluates the quantities

$$\Delta O_i^+ = \max\{O\left(\kappa_i = 1/2\right), O\left(\kappa_i = 1\right), O\left(\kappa_i = 2\right)\} - O\left(\kappa_i = 1\right),$$
$$\Delta O_i^- = \min\{O\left(\kappa_i = 1/2\right), O\left(\kappa_i = 1\right), O\left(\kappa_i = 2\right)\} - O\left(\kappa_i = 1\right). \tag{3}$$

In Eqs. (3) we introduced the quantities $\kappa_i = \mu_i/\mu_{i,0}$ where the index $i \in \{s, h, f\}$. The three quantities ΔO_i^+ (ΔO_i^-) are then combined in quadrature in order to obtain the scale uncertainty above (below) the central value.

The dependence of the physical predictions on the factorization, hard and soft scales is expected to become progressively smaller as more perturbative orders are added to fixed order calculations and a higher logarithmic accuracy is reached in resummed calculations. Since we obtain predictions at NLO+NLL accuracy, it is important to choose carefully the default values for the hard, soft and factorization scales. For all of the scales we choose dynamic default values depending on $t\bar{t}X_0$ invariant mass. With the method chosen for the resummation of the soft emission corrections the choice of the hard and soft scales is straightforward and is dictated by the kind of scale dependent logarithms found in the hard and soft function respectively. This leads to the choice $\mu_{h,0} = M$ and $\mu_{s,0} = M/\bar{N}$, where $\bar{N} = Ne^{\gamma_{\text{E}}}$ and N is the Mellin moment parameter while γ_{E} indicates the Euler-Mascheroni constant. For the SM case, the choice of a suitable central value for the factorization scale was discussed in [16]. The total $t\bar{t}H$ total cross section calculated as a function of μ_f at NLO, NLO+NLL and NLO+NNLL shows that these three curves intersect each other at $\mu_f/M \sim 0.5$ (see Fig. 1 in [16]) while the curves differ significantly for much smaller or much larger values of μ_f. This fact motivated the choice $\mu_{f,0} = M/2$ in [16]. The process considered in this work differs from the SM $t\bar{t}H$ production simply because of the presence of the pseudoscalar coupling in Eq. (1). Since the pseudoscalar coupling is not expected to change the scale behavior of the cross section, we set $\mu_{f,0} = M/2$ also in this work.

Finally, the calculations of the total cross section and differential distributions presented in the rest of this paper were obtained by employing the input parameters listed in Table I. The input parameters chosen are the same ones employed in [27]. Throughout the paper we

---

[1] For an introduction to the soft-collinear effective theory methods employed in this approach to partonic threshold resummation see for example [31].

M_W	80.419 GeV	m_t	173 GeV
M_Z	91.188 GeV	m_H	125 GeV
$1/\alpha$	137.036	$\alpha_s\,(M_Z)$	from MMHT 2014 PDFs

TABLE I: Input parameters employed throughout the calculation.

order	PDF order	α	σ [fb]
LO	LO	0	$378.7^{+120.6\,(32\%)}_{-85.2\,(22\%)}$
LO	LO	$\pi/2$	$142.4^{+50.1\,(35\%)}_{-34.6\,(24\%)}$
NLO	NLO	0	$475.0^{+47.3\,(10\%)}_{-51.9\,(11\%)}$
NLO	NLO	$\pi/2$	$192.4^{+23.3\,(12\%)}_{-24.3\,(13\%)}$
NLO+NLL	NLO	0	$480.3^{+57.8\,(12\%)}_{-15.6\,(3.2\%)}$
NLO+NLL	NLO	$\pi/2$	$199.6^{+17.7\,(8.9\%)}_{-8.4\,(4.2\%)}$

TABLE II: Total cross section for $t\bar{t}X_0$ production at the LHC with $\sqrt{s} = 13$ TeV and MMHT 2014 PDFs. The default value of the factorization scale is $\mu_{f,0} = M/2$, and the uncertainties are estimated through variations of this scale (and of the hard and soft scales μ_s and μ_h in resummed calculations).

order	PDF order	α	σ [fb]
NLO	NLO	0	$475.0^{+47.3\,(10\%)}_{-51.9\,(11\%)}$
NLO	NLO	$\pi/6$	$404.4^{+41.3\,(10\%)}_{-45.0\,(11\%)}$
NLO	NLO	$\pi/4$	$333.7^{+35.3\,(11\%)}_{-38.1\,(11\%)}$
NLO	NLO	$\pi/3$	$263.1^{+29.3\,(11\%)}_{-31.2\,(12\%)}$
NLO	NLO	$\pi/2$	$192.4^{+23.3\,(12\%)}_{-24.3\,(13\%)}$
NLO+NLL	NLO	0	$480.3^{+57.8\,(12\%)}_{-15.6\,(3.2\%)}$
NLO+NLL	NLO	$\pi/6$	$410.1^{+47.4\,(12\%)}_{-12.4\,(3.0\%)}$
NLO+NLL	NLO	$\pi/4$	$339.9^{+37.0\,(11\%)}_{-9.8\,(2.9\%)}$
NLO+NLL	NLO	$\pi/3$	$269.8^{+27.0\,(10\%)}_{-8.4\,(3.1\%)}$
NLO+NLL	NLO	$\pi/2$	$199.6^{+17.7\,(8.9\%)}_{-8.4\,(4.2\%)}$

TABLE III: Total cross section for $t\bar{t}X_0$ production at the LHC with $\sqrt{s} = 13$ TeV as a function of the angle α.

employ MMHT 2014 PDFs [33]; in particular, we employ LO PDFs in LO calculations and NLO PDFs in NLO and NLO+NLL calculations.

A. Total Cross Section

We start by discussing results for the total cross section. Table II lists values for the total cross section for the purely scalar coupling case ($\alpha = 0$) and for the purely pseudoscalar case ($\alpha = \pi/2$). The table reports numbers for LO, NLO and NLO+NLL calculations. The residual perturbative uncertainty is estimated by varying the factorization scale (in all calculations) and the hard and soft scales (in NLO+NLL calculations) as explained in the previous section. Table II shows that the NLO corrections increase significantly the central value of the total cross section for the two values of α considered. Furthermore, as expected, the NLO scale uncertainty is significantly smaller than the LO one. The resummation of soft emission corrections to NLL accuracy results into a small increase of the central value of the cross section, of the order of a few percent. The scale uncertainty interval obtained by varying the three scales in the resummed cross section is smaller than the scale uncertainty interval affecting the NLO calculation for both values of α. We notice that the resummation effect is larger for the purely pseudoscalar case than for the purely scalar one. This is due to the fact that in the purely pseudoscalar case the large invariant mass region contributes, in proportion, to a larger fraction of the total cross section with respect to the purely scalar case. This fact can

be noticed by looking at the invariant mass distribution shown in the upper-left plot of Figure 2. In the invariant mass tail the soft emission corrections dominate the cross section, hence resummation has larger effects in that region. The PDF uncertainty on the NLO results was evaluated separately by means of MG5_aMC by considering the MMHT2014nlo68cl PDF set. It is of the order or $\sim \pm 3\%$. The PDF uncertainty affecting the NLO+NLL result is expected to be of the same magnitude. Another source of uncertainty is related to the choice of top-quark mass used in the calculation. In the present work, we carry out all calculations in terms of the top quark pole mass. Another possible choice would be to use the $\overline{\text{MS}}$ running mass. An ab-initio calculation of the $t\bar{t}H$ cross section in terms of the running mass would require modifying several aspects of our calculation framework, including the NLO provider program which we employ. However one can get a sense of what the numerical impact of these different choices for the quark mass would be by looking at the results reported in [28] for the top pair production total cross section. There it is found that the use of the running mass enhances the total cross section by $\sim 10\%$ at NLO with respect to a calculation employing the pole mass. The effect of this mass scheme change is only $\sim 1\%$ at approximate NNLO (essentially, the latter is obtained by re-expanding NNLL resummation formula). Therefore, it is reasonable to expect that the uncertainty associated to the choice of the top-quark mass scheme would have an impact of a few percent on the NLO+NLL calculation discussed in this work.

Finally, we checked that in NLO calculations an independent variation of μ_f and μ_r around the value $M/2$ leads to the same scale uncertainties reported in Table II, which was obtained by setting $\mu_f = \mu_r$ from the start.

The result for other values of the mixing angle α can be obtained by employing the relation

$$\sigma(\alpha) = \sigma_H \cos^2\alpha + \sigma_A \sin^2\alpha \,. \qquad (4)$$

In Eq. (4), σ_H indicates the total cross section for a pure SM like coupling, while σ_A indicates the cross section for a pure pseudoscalar coupling. At NLO, the scale uncertainty at an arbitrary angle can be obtained in a similar way by exploiting the fact that the upper edge of the scale uncertainty band corresponds to the NLO calculation in which the factorization scale is set equal to $\mu_{f,0}/2$, while the lower edge corresponds to the calculation in which one sets $\mu_f = 2\mu_{f,0}$. Eq. (4) can also be employed to obtain the central value of the NLO+NLL cross section at an arbitrary angle. However, since the estimate of the scale uncertainty at NLO+NLL accuracy involves the independent variation of three scales, it cannot be obtained directly from the results of Table II and it must be evaluted separately. Table III lists the values of the NLO and NLO+NLL cross section and of their scale uncertianty for a few values of the angle α. Figure 1 shows the dependence of the total cross-section on the mixing angle. For all values of α the NLO+NLL cross section is a few femtobarn higher than the NLO one, while the scale uncertainty intervals at NLO+NLL are slightly smaller than the corresponding NLO intervals.

B.   Differential Distributions

Our goal is to see if the four distributions listed in the introduction, and in particular their shapes, are sensitive to the scalar and/or pseudoscalar nature of the X_0 coupling. As for the total cross section, we consider here the case $\alpha = 0$ (SM-like Higgs boson) and $\alpha = \pi/2$ (pure pseudoscalar coupling). The value of the differential distributions for arbitrary α can be obtained by combining the distribution at $\alpha = 0$ and $\alpha = \pi/2$ as in Eq. (4) for the case of the total cross section. In addition, we want to check if the shape of these distributions is stable with respect to the inclusion of soft gluon emission corrections through the resummation process.

These differential distributions evaluated to NLO with `MG5_aMC` are shown in Figure 2. The bands represent the residual perturbative uncertainty evaluated through the variation of the factorization scale as explained above. At this stage, we made no attempt to account for the PDFs uncertainty. The bottom part of each panel shows the width of the uncertainty band in each bin divided by its central value, and allows one to assess the relative scale uncertainty of the bands for the scalar and pseudoscalar cases. We see that the relative scale uncertainties for the cases $\alpha = 0$ and $\alpha = \pi/2$ are very similar.

The distributions presented in Figure 3 are the same distributions shown in Figures 2 but this time they are evaluated to NLO+NLL accuracy. The scale uncertainty bands in Figure 3 are slightly narrower than the ones at NLO (shown in Figure 2) as a consequence of the inclusion of resummed soft gluon emission corrections. Figure 4 shows the distributions at NLO+NLL normalized to their total cross section, i.e. the height of each bin is divided by the total cross section. Consequently, the

sum of the height of all bins in each distribution (including the ones outside the range shown in the figure) is equal to 1. The scale uncertainty bands become extremely thin. For this reason we decided to show only the central value ($\mu_f = M/2$, $\mu_h = M$, $\mu_s = M/\bar{N}$) for both the scalar and the pseudoscalar case. By examining Figure 4 one sees that, with the exception of the p_T^t differential distribution, the shape of the normalized distributions in the scalar and pseudo-scalar cases is quite different. In the M, $M_{t\bar{t}}$ and p_T^X distributions, the peak of the scalar coupling distribution is more pronounced and shifted to the left with respect to the peak of the pseudoscalar coupling distribution. As mentioned in the Introduction, the shape difference between distributions with scalar and pesudoscalar couplings can be experimentally used to probe the pseudoscalar component of the Yukawa coupling.

One might wonder if there is a difference in shape between the fixed order and the matched distributions. It turns out that the NLO normalized distributions are extremely similar to the ones in Figure 4 because the resummed soft emission corrections have a small impact on the shape of the distributions in the ranges of values of M, $M_{t\bar{t}}$, p_T^t and p_T^X shown in the figure. This can be seen in Figure 5, which shows the ratio of the normalized distributions at NLO+NLL over the normalized distributions evaluated to NLO. The relative difference between these distributions is consistently smaller than a few percent. We checked that for all distributions considered, the NLO+NLL bands shown in Figure 3 consistently overlap with the upper part of the corresponding NLO bands shown in Figure 2. This behavior is similar to the one observed for the associated production of a top quark pair with a W boson [29] and the associated production of a top quark pair with a Z boson [30]. As expected, resummation effects are most relevant in the tail of the pair invariant mass distribution. This can be seen by looking at Figure 6 which shows the NLO and NLO+NLL distributions in the case in which the uncertainty band in each bin is divided by the central value of the NLO+NLL bin. This behavior is expected since high values of the invariant mass correspond to partonic events with less energy available for the production of hard gluons. Notice that Figure 6 covers a larger range of values of M with respect to the previous figures; the resummation will have an impact on the shape of the distribution for large values of M.

III.   EXPERIMENTAL MOTIVATION

The cross-section for the $t\bar{t}X_0$ production channel has a very simple dependence on the mixing angle. This implies that the calculation of the cross section in the pure scalar case, σ_H, and in the pure pseudoscalar case, σ_A, allows us to fully reconstruct the dependence for any arbitrary α. Therefore, the measurement of the total cross section by itself allows one to probe the pseudoscalar

component of the top quark Yukawa coupling. This dependence on the mixing angle is also true for the aforementioned differential cross section distributions in any particular bin. As a result, the expected uncertainty on $|\cos\alpha|$ can be easily calculated as a function of the cross section. In the SM scenario, assuming an hypothetical cross section measurement of $\sigma = \sigma_H \pm \Delta\sigma$, one finds

$$
\begin{aligned}
\Delta|\cos\alpha| &= \frac{\partial|\cos\alpha|}{\partial\sigma}\Delta\sigma \\
&= \frac{1}{2}\frac{1}{\sigma_H - \sigma_A}\Delta\sigma \\
&\approx 0.86^{+0.09}_{-0.03}\left(\frac{\sigma_H}{\Delta\sigma}\right)^{-1},
\end{aligned}
\tag{5}
$$

according to Table II, at NLO+NLL. The uncertainty on $|\cos\alpha|$ is inversely proportional to the statistical significance of the production channel. The graphical representation of the lower limit on $\cos\alpha$ at 68.3% CL with the statistical significance of the SM Higgs boson associated production with a top quark pair is presented in Figure 7. An eventual five sigma observation of this channel, in the SM hypothesis, would set a limit of $|\cos\alpha| > 0.83^{+0.01}_{-0.02}$ at 68.3% CL, growing asymptotically to one with the increase of significance. The error on this limit, represented by the blue shaded band in Figure 7, emerges from the uncertainty on the cross-sections in Table II due to scales variations.

The theoretical uncertainty on the $t\bar{t}X_0$ signal cross section, in particular the scale dependence, comprises one of the components of the full systematic error taken into account in experimental measurements at the LHC. The observed improvement on the scale uncertainty at NLO+NLL is expected to significantly decrease the impact of the scale dependences on the Monte Carlo signal estimation, and therefore, on the overall systematic error [34]. Moreover, the k-factors associated with the ratio of the NLO+NLL cross section with respect to the NLO calculation,

$$
k = \sigma^{\text{NLO+NLL}}/\sigma^{\text{NLO}},
\tag{6}
$$

range from 1.010 to 1.012 (1.048 to 1.025) for the transverse momentum of the top quark in the pure scalar (pseudoscalar) scenario, as can be seen in Figure 8. This information is useful to reweight the simulated transverse momenta of the top quark and X_0 boson in the experimental measurement analyses, for any specific mixture of the two components. The theoretical understanding of the shapes of the transverse momentum and invariant mass distributions is also extremely important for the full kinematic reconstruction of $t\bar{t}X_0$ dilepton events, and they can also be used in experimental analyses to repair the distortion caused by the detector response, kinematic cuts applied in the trigger and in the offline event reconstruction and selection.

IV. CONCLUSIONS

In this work we studied the associated production of a top-antitop pair and a scalar X_0 which is allowed to couple to the top quark current with a mixture of scalar and pseudoscalar couplings. The scalar coupling is the SM Yukawa coupling modulated by a factor $\cos\alpha$, where α is the angle which parameterizes the relative strength of the scalar and pseudoscalar components of the coupling. We evaluated the total cross section for this process for the special cases $\alpha = 0$ (SM Higgs) and $\alpha = \pi/2$ (pure pseudoscalar coupling) to NLO+NLL accuracy, where the NLL resummation was carried out in the soft gluon emission limit. We showed that it is straightforward to use this information in order to evaluate the total cross section for arbitrary values of α.

Recent studies point to the possibility of a reliable kinematic reconstruction of the top, antitop and X_0 momenta. For this reason, we studied differential distributions with respect to the final state invariant mass, X_0 transverse momentum, top-pair invariant mass and top-quark transverse momentum to NLO+NLL accuracy. By comparing the $\alpha = 0$ and $\alpha = \pi/2$ cases, we showed that the shapes of the first three distributions listed above depend quite strongly on the scalar or pseudoscalar nature of the coupling between the top quark and the Higgs boson. In addition, these shapes are stable with respect to the inclusion of higher-order soft emission corrections. Results for the distributions at arbitrary values of α can be easily obtained by considering an appropriate bin-by-bin combination of the results at $\alpha = 0$ and $\alpha = \pi/2$.

It is shown that a possible future observation of the associated production of a top quark pair with a Higgs boson in the SM hypothesis could immediately establish a limit on the pseudoscalar component of the top quark Yukawa coupling of $|\cos\alpha| > 0.83^{+0.01}_{-0.02}$, at 68.3% CL. Moreover, a full kinematic reconstruction of the final state momenta for this process could provide valuable information by means of angular distributions and asymmetries, which can be combined with the cross section result. The theoretical understanding of the aforementioned differential kinematic distributions is also extremely useful for the experimental measurement itself, as they can provide k-factors for transverse momentum reweighting, and probability density functions for neutrino reconstruction in dilepton events.

[1] W. Beenakker, S. Dittmaier, M. Kramer, B. Plumper, M. Spira and P. M. Zerwas, Phys. Rev. Lett. **87**, 201805 (2001) doi:10.1103/PhysRevLett.87.201805 [hep-ph/0107081].

[2] W. Beenakker, S. Dittmaier, M. Kramer, B. Plumper, M. Spira and P. M. Zerwas, Nucl. Phys. B **653**, 151 (2003) doi:10.1016/S0550-3213(03)00044-0 [hep-ph/0211352].

[3] L. Reina, S. Dawson and D. Wackeroth, Phys. Rev. D **65**, 053017 (2002) doi:10.1103/PhysRevD.65.053017 [hep-ph/0109066].

[4] L. Reina and S. Dawson, Phys. Rev. Lett. **87**, 201804 (2001) doi:10.1103/PhysRevLett.87.201804 [hep-ph/0107101].

[5] S. Dawson, L. H. Orr, L. Reina and D. Wackeroth, Phys. Rev. D **67**, 071503 (2003) doi:10.1103/PhysRevD.67.071503 [hep-ph/0211438].

[6] S. Dawson, C. Jackson, L. H. Orr, L. Reina and D. Wackeroth, Phys. Rev. D **68**, 034022 (2003) doi:10.1103/PhysRevD.68.034022 [hep-ph/0305087].

[7] R. Frederix, S. Frixione, V. Hirschi, F. Maltoni, R. Pittau and P. Torrielli, Phys. Lett. B **701**, 427 (2011) doi:10.1016/j.physletb.2011.06.012 [arXiv:1104.5613 [hep-ph]].

[8] M. V. Garzelli, A. Kardos, C. G. Papadopoulos and Z. Trocsanyi, Europhys. Lett. **96**, 11001 (2011) doi:10.1209/0295-5075/96/11001 [arXiv:1108.0387 [hep-ph]].

[9] Y. Zhang, W. G. Ma, R. Y. Zhang, C. Chen and L. Guo, Phys. Lett. B **738**, 1 (2014) doi:10.1016/j.physletb.2014.09.022 [arXiv:1407.1110 [hep-ph]].

[10] S. Frixione, V. Hirschi, D. Pagani, H. S. Shao and M. Zaro, JHEP **1409**, 065 (2014) doi:10.1007/JHEP09(2014)065 [arXiv:1407.0823 [hep-ph]].

[11] S. Frixione, V. Hirschi, D. Pagani, H.-S. Shao and M. Zaro, JHEP **1506**, 184 (2015) doi:10.1007/JHEP06(2015)184 [arXiv:1504.03446 [hep-ph]].

[12] H. B. Hartanto, B. Jager, L. Reina and D. Wackeroth, Phys. Rev. D **91**, no. 9, 094003 (2015) doi:10.1103/PhysRevD.91.094003 [arXiv:1501.04498 [hep-ph]].

[13] A. Denner and R. Feger, JHEP **1511**, 209 (2015) doi:10.1007/JHEP11(2015)209 [arXiv:1506.07448 [hep-ph]].

[14] A. Denner, J. N. Lang, M. Pellen and S. Uccirati, JHEP **1702**, 053 (2017) doi:10.1007/JHEP02(2017)053 [arXiv:1612.07138 [hep-ph]].

[15] A. Broggio, A. Ferroglia, B. D. Pecjak, A. Signer and L. L. Yang, JHEP **1603**, 124 (2016) doi:10.1007/JHEP03(2016)124 [arXiv:1510.01914 [hep-ph]].

[16] A. Broggio, A. Ferroglia, B. D. Pecjak and L. L. Yang, JHEP **1702**, 126 (2017) doi:10.1007/JHEP02(2017)126 [arXiv:1611.00049 [hep-ph]].

[17] A. Kulesza, L. Motyka, T. Stebel and V. Theeuwes, JHEP **1603**, 065 (2016) doi:10.1007/JHEP03(2016)065 [arXiv:1509.02780 [hep-ph]].

[18] A. Kulesza, L. Motyka, T. Stebel and V. Theeuwes, PoS LHCP **2016**, 084 (2016) [arXiv:1609.01619 [hep-ph]].

[19] A. Kulesza, L. Motyka, T. Stebel and V. Theeuwes, arXiv:1704.03363 [hep-ph].

[20] J. Alwall *et al.*, JHEP **1407**, 079 (2014) doi:10.1007/JHEP07(2014)079 [arXiv:1405.0301 [hep-ph]].

[21] G. Aad *et al.* [ATLAS Collaboration], JHEP **1605**, 160 (2016) doi:10.1007/JHEP05(2016)160 [arXiv:1604.03812 [hep-ex]].

[22] V. Khachatryan *et al.* [CMS Collaboration], JHEP **1409**, 087 (2014) Erratum: [JHEP **1410**, 106 (2014)] doi:10.1007/JHEP09(2014)087, 10.1007/JHEP10(2014)106 [arXiv:1408.1682 [hep-ex]].

[23] G. Aad *et al.* [ATLAS and CMS Collaborations], JHEP **1608**, 045 (2016) doi:10.1007/JHEP08(2016)045 [arXiv:1606.02266 [hep-ex]].

[24] F. Demartin, F. Maltoni, K. Mawatari, B. Page and M. Zaro, Eur. Phys. J. C **74**, no. 9, 3065 (2014) doi:10.1140/epjc/s10052-014-3065-2 [arXiv:1407.5089 [hep-ph]].

[25] P. Artoisenet *et al.*, JHEP **1311**, 043 (2013) doi:10.1007/JHEP11(2013)043 [arXiv:1306.6464 [hep-ph]].

[26] S. P. Amor dos Santos *et al.*, Phys. Rev. D **92**, no. 3, 034021 (2015) doi:10.1103/PhysRevD.92.034021 [arXiv:1503.07787 [hep-ph]].

[27] S. Amor Dos Santos *et al.*, Phys. Rev. D **96**, no. 1, 013004 (2017) doi:10.1103/PhysRevD.96.013004 [arXiv:1704.03565 [hep-ph]].

[28] V. Ahrens, A. Ferroglia, M. Neubert, B. D. Pecjak and L. L. Yang, Phys. Lett. B **703**, 135 (2011) doi:10.1016/j.physletb.2011.07.058 [arXiv:1105.5824 [hep-ph]].

[29] A. Broggio, A. Ferroglia, G. Ossola and B. D. Pecjak, JHEP **1609**, 089 (2016) doi:10.1007/JHEP09(2016)089 [arXiv:1607.05303 [hep-ph]].

[30] A. Broggio, A. Ferroglia, G. Ossola, B. D. Pecjak and R. D. Sameshima, JHEP **1704**, 105 (2017) doi:10.1007/JHEP04(2017)105 [arXiv:1702.00800 [hep-ph]].

[31] T. Becher, A. Broggio and A. Ferroglia, Lect. Notes Phys. **896**, pp.1 (2015) doi:10.1007/978-3-319-14848-9 [arXiv:1410.1892 [hep-ph]].

[32] S. Catani, M. L. Mangano, P. Nason and L. Trentadue, Nucl. Phys. B **478**, 273 (1996) doi:10.1016/0550-3213(96)00399-9 [hep-ph/9604351].

[33] L. A. Harland-Lang, A. D. Martin, P. Motylinski and R. S. Thorne, Eur. Phys. J. C **75**, no. 5, 204 (2015) doi:10.1140/epjc/s10052-015-3397-6 [arXiv:1412.3989 [hep-ph]].

[34] CMS Collaboration [CMS Collaboration], CMS-PAS-HIG-16-038.

[35] G. Aad *et al.* [ATLAS Collaboration], JHEP **1206**, 088

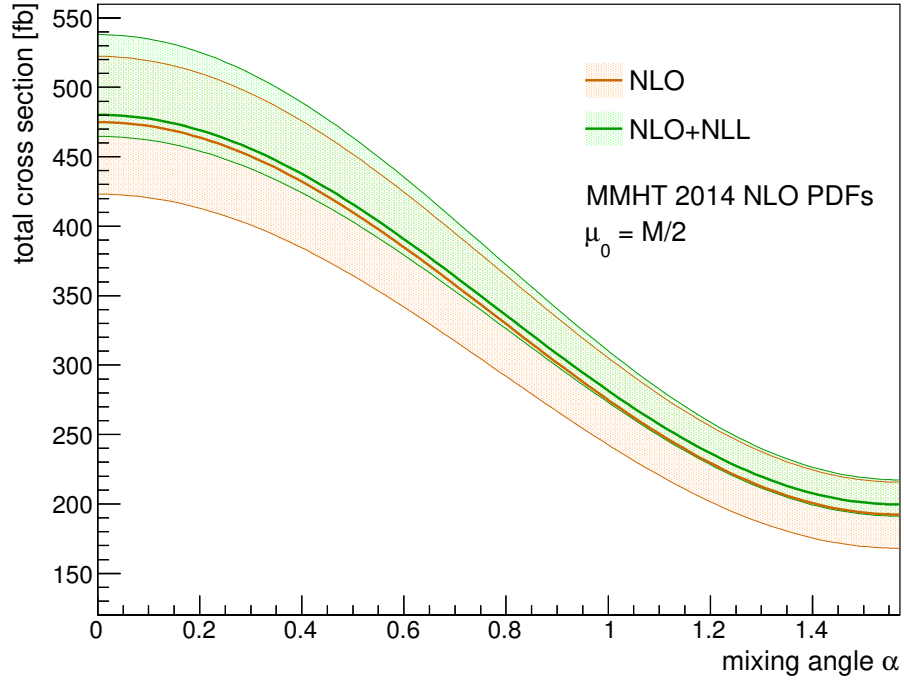(2012) doi:10.1007/JHEP06(2012)088 [arXiv:1205.2484 [hep-ex]].

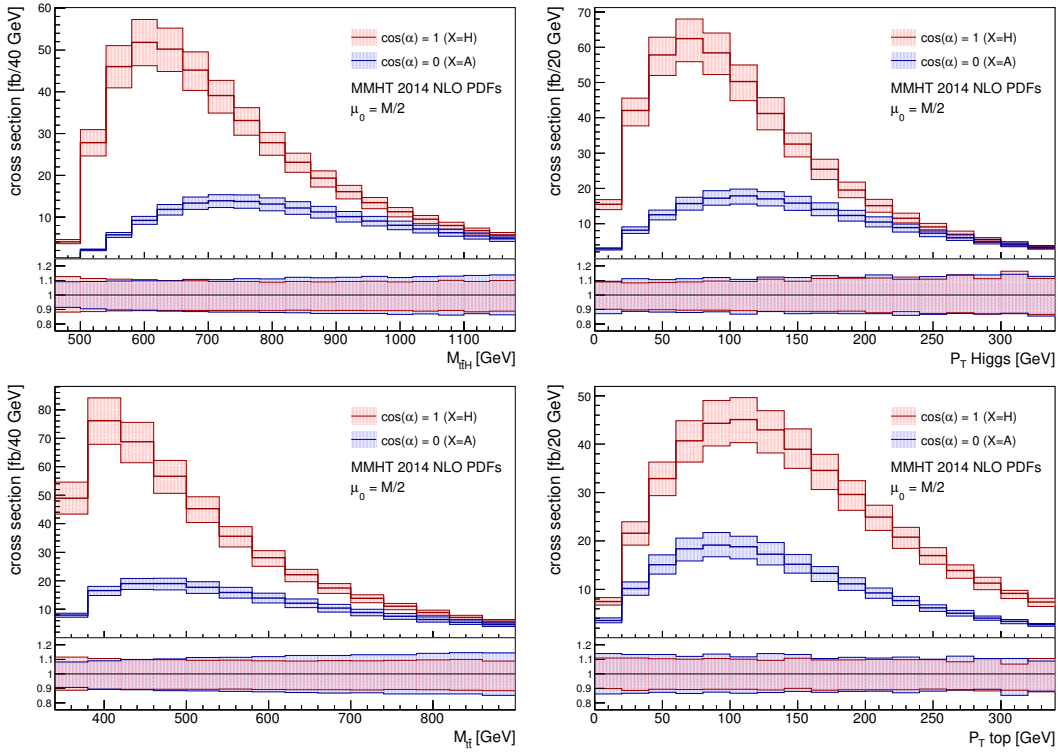FIG. 1: Dependence of the total cross-section on the mixing angle α.

FIG. 2: Differential distributions evaluated at NLO. The default factorization scale is chosen as $\mu_{f,0} = M/2$, and the uncertainty bands are generated through scale variations as explained in the text.
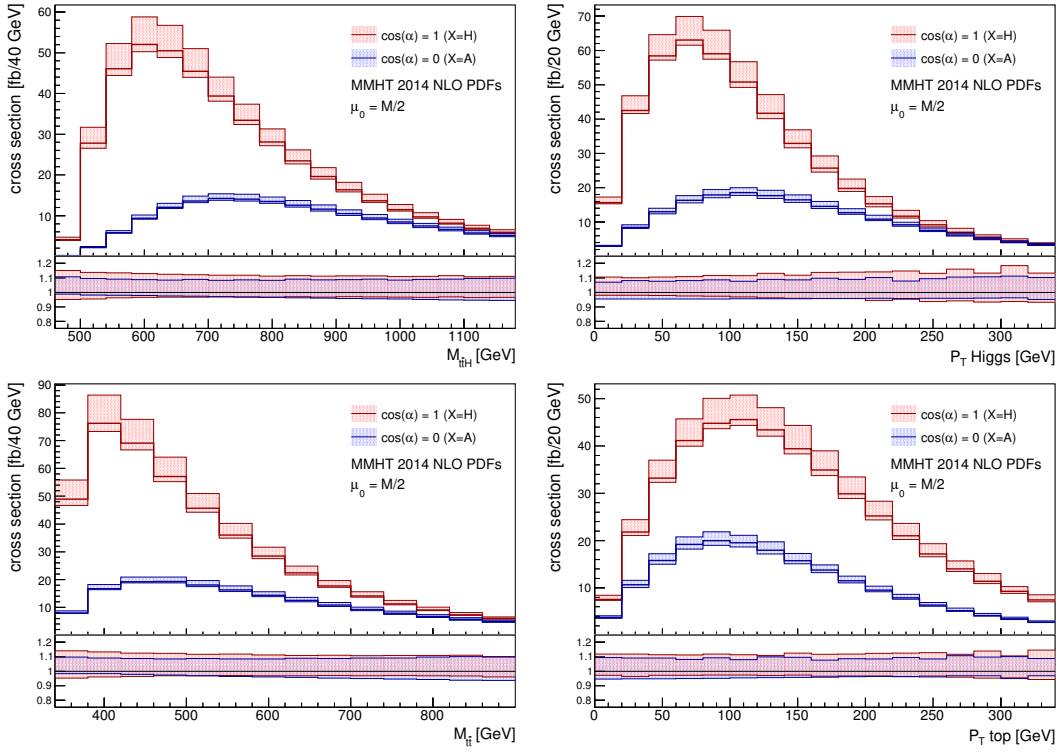
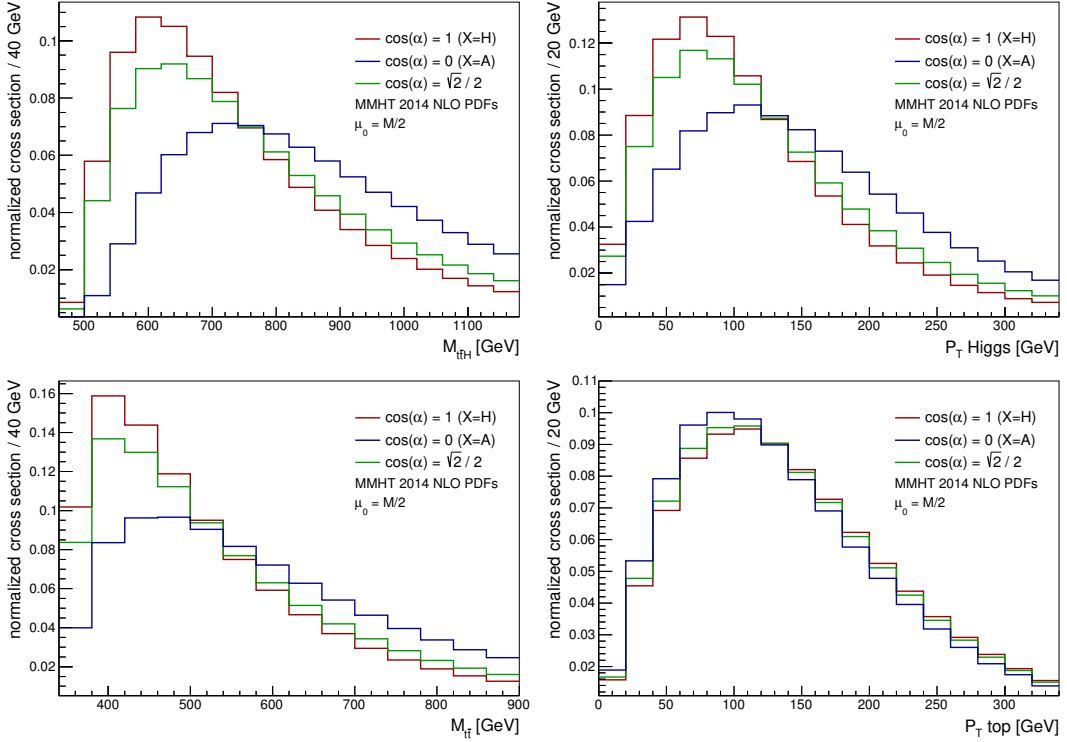FIG. 3: Differential distributions evaluated at NLO+NLL. The uncertainty bands are generated through scale variations as explained in the text.

FIG. 4: Normalized differential distributions evaluated at NLO+NLL. The factorization scale is set to $\mu_f = M/2$.
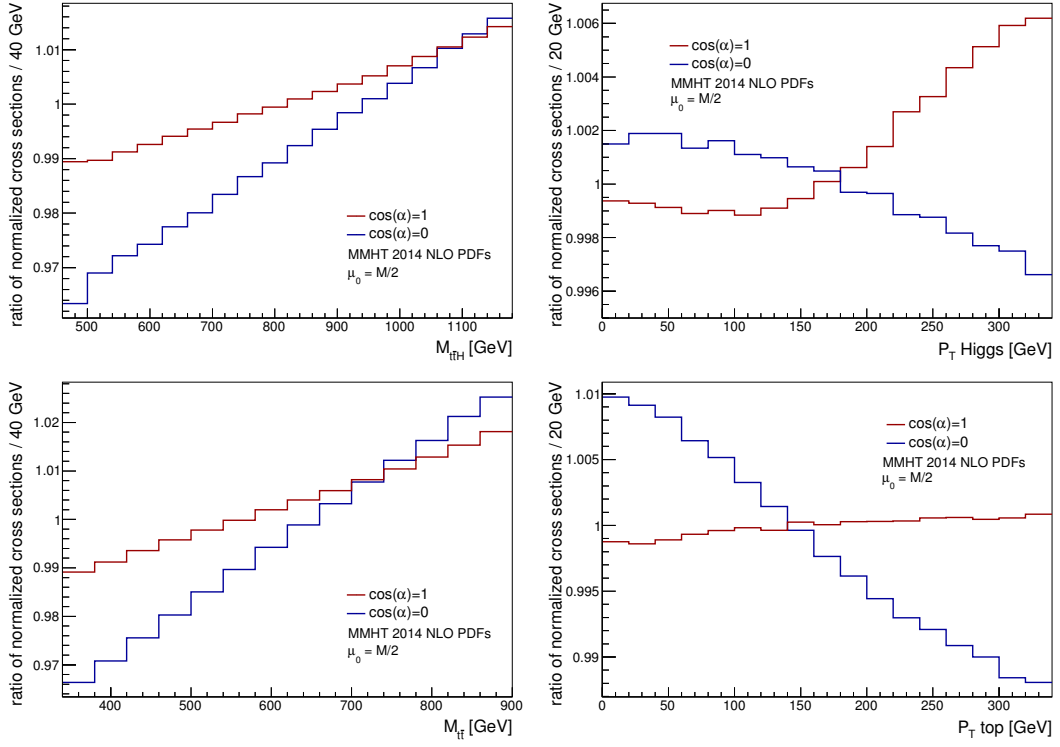
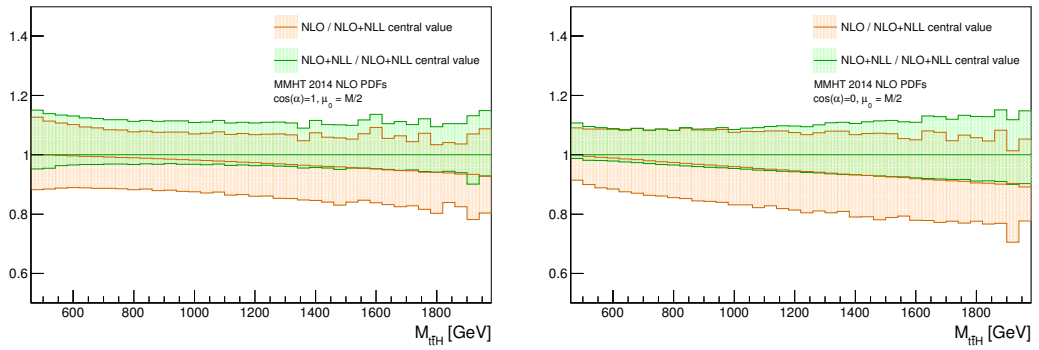FIG. 5: Ratio of the normalized distributions at NLO+NLL over NLO distributions.

FIG. 6: $t\bar{t}H$ invariant mass distributions: For each bin, the figure shows the ratio of the differential cross section at NLO+NLL and NLO over the central value of the NLO+NLL bin.
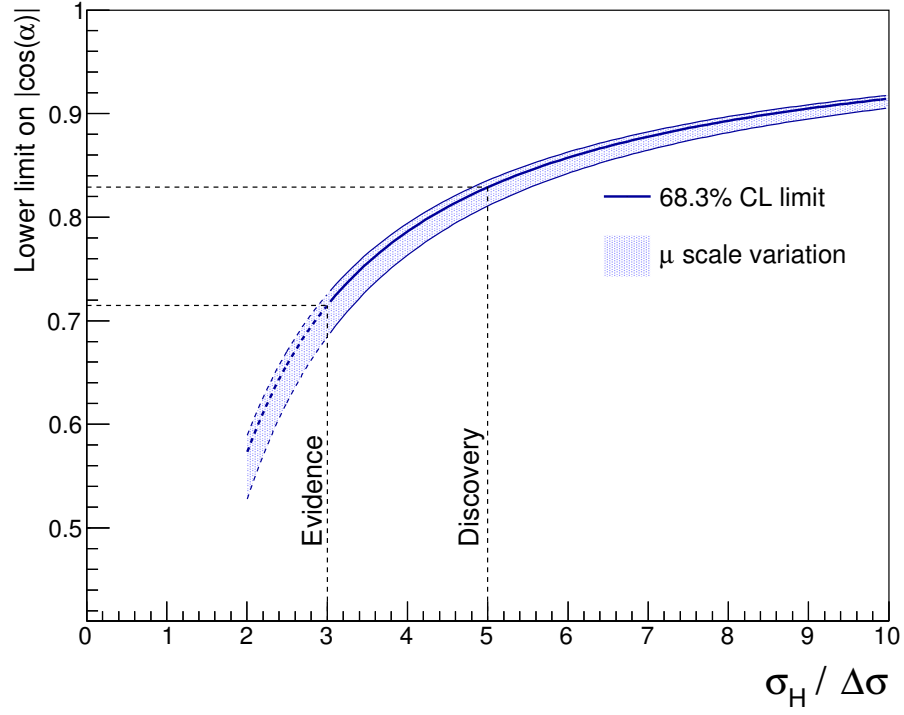
FIG. 7: Dependence of the lower limit on $|\cos(\alpha)|$ at 68.3% CL with the statistical significance of the SM Higgs boson associated production with a top quark pair, at NLO+NLL. The blue error band around the central limit line represents the scale uncertainty.
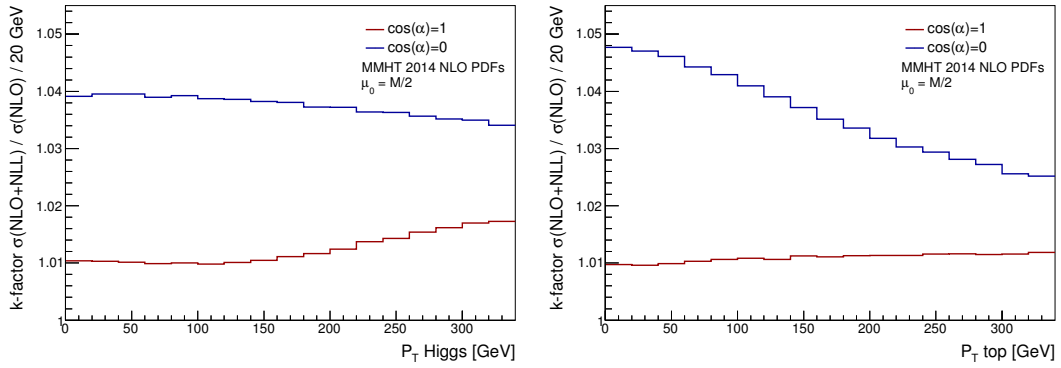

FIG. 8: Ratio of the cross-section at NLO+NLL over NLO distributions (k-factors).